MASTERARBEIT | MASTER'S THESIS

Titel | Title

Developing a suitable metabolite analysis protocol for the (R)-[11C]Me-NB1 PET-radiotracer in NMDA receptor research

verfasst von | submitted by

Dott. mag. Diana Brancadoro

angestrebter akademischer Grad | in partial fulfilment of the requirements for the degree of

Master of Science (MSc)

Wien | Vienna, 2024

Studienkennzahl lt. Studienblatt | Degree programme code as it appears on the student record sheet:	UA 066 606
Studienrichtung lt. Studienblatt | Degree programme as it appears on the student record sheet:	Masterstudium Drug Discovery and Development
Betreut von | Supervisor:	Prof. Dr. Rupert Lanzenberger

Abstract

The study delves into the molecular complexities of ionotropic glutamate receptors, particularly focusing on N-methyl-D-aspartate receptors (NMDARs) and their pivotal role in neurological and psychiatric disorders. By scrutinizing the intricate structure and function of NMDARs, the research elucidates their involvement in various pathophysiological processes. Moreover, the investigation explores the application of positron emission tomography (PET) in understanding NMDAR-related pathologies, offering insights into potential therapeutic interventions.

A primary objective of the study is the optimization and validation of a simplified chromatographic method via solid-phase extraction for metabolite correction from arterial blood samples, specifically analysing the radioligand *(R)*-[^{11}C]Me- NB1. Through iterative experimental approaches, the method achieves enhanced accuracy and reliability compared to conventional high-performance liquid chromatography (HPLC) techniques. Leveraging solid-phase extraction with C-18 cartridges, the study establishes a robust foundation for further refinement and validation of the method.

Additionally, the project endeavours to develop a standard operating procedure (SOP) for planned *(R)*-[^{11}C]Me-NB1 studies, aiming to facilitate its application in clinical settings, particularly at the General Hospital of the Medical University of Vienna, Department of Biomedical Imaging and Image-guided Therapy, Division of Nuclear Medicine.

By elucidating the molecular intricacies of NMDARs and refining analytical methodologies for radioligand studies, this research contributes to advancements in neuroimaging and drug development for neurological and psychiatric disorders. The study underscores the significance of meticulous methodological approaches

and emphasizes the potential of PET in unrevealing the complexities of neurotransmitter systems in the central nervous system.

Abstrakt

Die Studie untersucht die molekularen Komplexität von ionotropen Glutamatrezeptoren, insbesondere die N-Methyl-D-Aspartat-Rezeptoren (NMDARs) und ihre entscheidende Rolle bei neurologischen und psychiatrischen Störungen. Durch die gründliche Untersuchung der komplizierten Struktur und Funktion von NMDARs erläutert die Forschung ihre Beteiligung an verschiedenen pathophysiologischen Prozessen. Darüber hinaus erforscht die Untersuchung die Anwendung der Positronemissionstomographie (PET) beim Verständnis von NMDAR-bezogenen Pathologien und bietet Einblicke in mögliche therapeutische Interventionen.

Ein Hauptziel der Studie ist die Optimierung und Validierung einer vereinfachten chromatographischen Methode mittels Solidphase-Extraktion zur Metabolitkorrektur aus arteriellen Blutproben, insbesondere die Analyse des Radioligands (R)-[11C]Me-NB1. Durch iterative experimentelle Ansätze erreicht die Methode höhere Genauigkeit und Zuverlässigkeit im Vergleich zu herkömmlichen Hochleistungsflüssigchromatographie (HPLC) Techniken. Durch den Einsatz von Solid-Phase-Extraktionen mit C-18-Kassetten schafft die Studie eine solide Grundlage für die weitere Verfeinerung und Validierung der Methode.

Zusätzlich bemüht sich das Projekt um die Entwicklung eines Standardbetriebsverfahrens (SOP) für geplante (R)-[11C]Me-NB1-Studien, mit dem Ziel, seine Anwendung in klinischen Umgebungen zu erleichtern, insbesondere im Generalkrankenhaus der Medizinischen Universität Wien, Abteilung für biomedizinische Bildgebung und bildgesteuerte Therapie, Division für Nuklearmedizin.

Durch die Klärung der molekularen Komplexität von NMDARs und die Verfeinerung analytischer Methoden für Radioligand-Studien trägt diese Forschung zu Fortschritten in der Neuroimaging- und Medikamentenentwicklung

für neurologische und psychiatrische Störungen bei. Die Studie unterstreicht die Bedeutung sorgfältiger methodischer Ansätze und betont das Potenzial von PET, die Komplexität von Neurotransmittersystemen im zentralen Nervensystem zu enthüllen.

Acknowledgement

I would like to thank my supervisor, Prof. Dr. Rupert Lanzenberger, for the opportunity to work under his guidance and on this project.

My thankfulness also goes to Dr. Lukas Nics and Dr. Marius Ozenil for the continous support and the lessons given along the way.

I want to express my gratitude to Lisa, who has taugh me everything there is to know in a radiochemistry laboratory.

Thank you to Prof. Verena Pichler for her immense support and advice during this time.

Last but not least, a special thank you goes to my family for making this possible and Luca.

Table of Contents

List of Figures

Figure 11. The last set-up used (30/70 ACN/AmAc (pH 9)), shows on the chromatogram a satisfactory starting point for the study of the separation between *(R)*-[^{11}C]Me-NB1 and its metabolites.

List of Tables

Abbreviations

ACN	Acetonitrile
ADME	Absorption, distribution, metabolism, excretion
AMPAR	α-amino-3-hydroxy-5-methyl-4-isoxazolepropionic acid receptor
ATD	Amino-terminal domain
BBB	Blood-brain barrier
CNS	Central nervous system
CT	Computed tomography
CTD	Carboxyl terminal domain
HPLC	High-performance liquid chromatography
HLB	Hydrophilic-lipophilic-balanced
iGluRs	Ionotropic glutamate receptors
LBD	Ligand-binding domain
LPT	Long-term potentiation
LOD	Limit of detection
LTD	Long-term depression
mGluRs	G-protein-coupled metabotropic glutamate receptors
MRI	Magnetic resonance imaging
NMDAR	N-methyl-D-aspartate receptor
OPTCL	Micellar chromatography
PET	Positron emission tomography
PP	Polypropylene

QC	Quality control
SOP	Standard operating procedure
TLC	Thin-layer chromatography
TMD	Transmembrane domain
UV	Ultraviolet
WB	Whole blood
WS	Washing solution

INTRODUCTION

In the central nervous system (CNS) most of the excitatory neurotransmission is moderated by vesicular glutamate release. The receptors activated by this molecule can be divided into two groups: G-protein–coupled metabotropic glutamate receptors (mGluRs) and ionotropic glutamate receptors (iGluRs). iGluRs functions are important for several processes in the brain, spinal cord, and peripheral nervous system. Therefore, in numerous neurological and psychiatric diseases the dysregulation of iGluRs functions plays a fundamental role[3]. Ionotropic glutamate receptors are characterized by extensive molecular complexity, and they can be divided into three classes: α-amino-3-hydroxy-5-methyl-4-isoxazolepropionic acid receptors (AMPARs), NMDA, Kainate receptors (KainateRs). Since they are all named after the activating agonist, NMDAR is named after N-methyl-D-aspartate [4].

NMDA receptors and related pathophysiological processes

The NMDARs are tetrameric-membrane proteins composed of four subunits, forming a central ion channel, which means that they are heterotetrametric voltage-dependent receptors. This class of receptors is provided with unique characteristics such as high permeability to Ca^{2+} and extracellular Mg^{2+} blockage-responsive voltage variations [5,6].

Structurally, NMDAR can be formed with the assemblance of four out of seven subunits: GluN1, GluN2A-D, GluN3A, and GluN3B. These last two subunits are predominantly expressed in the prenatal and perinatal phase, therefore, they will not be deeply investigated from now on[7,8]. NMDAR quaternary structure is composed of four domains: an amino-terminal domain (ATD), an extracellular ligand-binding domain (LBD), and a transmembrane domain (TMD), and the carboxyl-terminal domain (CTD), also known as intracellular C-tail (Figure 1).

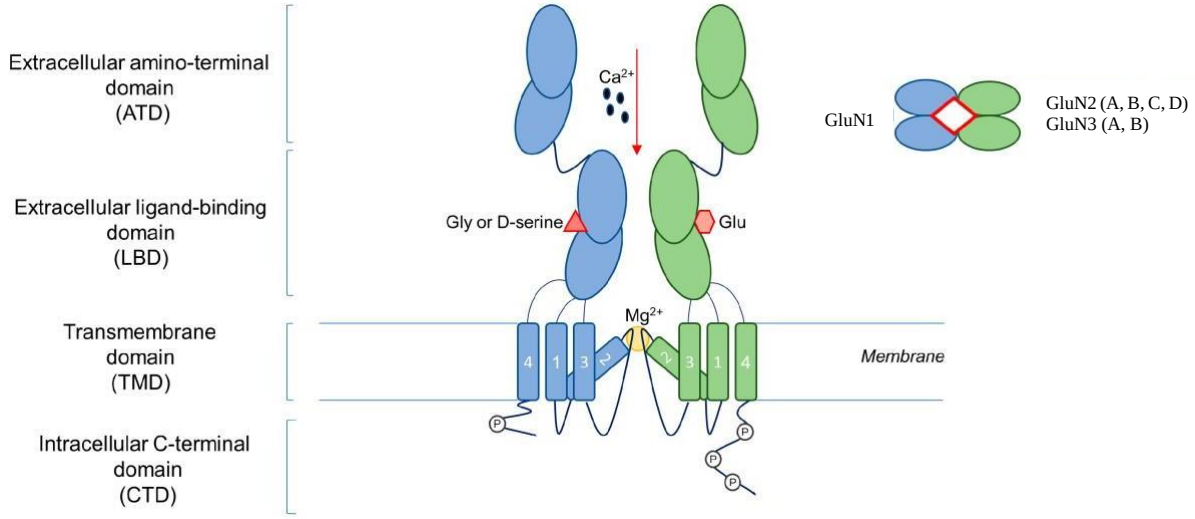

Figure 1. Schematic structure of NMDARs.[1] The transmembrane receptor is constituted by two GluN1 subunits and two GluN2 or GluN3 subunits, forming a heterotetrametric structure. An extracellular amino-terminal domain (ATD), an extracellular ligand-binding domain (LBD), a transmembrane domain (TMD), and an intracellular C-terminal domain (CTD) define NMDARs. (Image modified from Gallo, 2023)

The four glutamate-binding GluN2 subunits are products of different genes and assemble with two glycine-binding GluN1 to produce NMDAR with significantly divergent pharmacological properties and biological functions [9].

The ionotropic activation of NMDAR requires the synergy of interactions and modifications. Two molecules of glutamate bind on the GluN2 or GluN3 subunits, two molecules of glycine or D-serine, functioning as co-agonists, on the GluN1 subunits, and the Mg^{2+} channel blocker is removed[10]. In the ionotropic pathway, Ca^{2+} is allowed to enter the activated NMDA channels.

In the CNS, the Ca^{2+} penetration activates downstream intracellular signalling, inducting two major functions of synaptic plasticity: long-term potentiation (LPT) and long-term depression (LTD). These long-term activities regulating the synaptic transmission are participating in numerous pathophysiological processes[11].

NMDARs can be distinguished as synaptic and extrasynaptic receptors. While synaptic NMDARs are mainly associated with protective processes, extrasynaptic NMDARs, enriched in GluN2B subunits, when activated, may trigger cytotoxic

mechanisms[12]. Extrasynaptic NMDARs are enriched in GluN2B subunits, which are among the most abundant types in the adult forebrain. As the brain develops, their expression declines [13,14].

The variety of GluN2 subunits imparts different properties to the receptor but consequently, from their dysfunction, various diseases are attributed to the NMDAR[15]. Excessive NMDA receptor opening is responsible for acute elevated Ca^{2+} concentrations, which induce excitotoxic processes. Excitotoxicity mechanisms are followed by apoptosis and these processes are involved in acute traumatic brain injury, intoxications, ischemic processes, and stroke. The mechanisms induced by the elevated Ca^{2+} concentrations, also play a crucial role in the pathogenesis of chronic neurodegenerative disorders such as Huntington's, Parkinson's, and Alzheimer's diseases as well as depression or drug dependence[14,16].

Radioligands and PET

The development of drugs treating these disorders is commonly known as a growing field as the biology of most of the diseases is still not well understood. Positron emission tomography (PET) is a potent technology that has already significantly improved the knowledge of the pathophysiology of many CNS disorders, by observing alterations in the expression of neuroreceptors a disease is occurring [17]. PET non-invasive technology enables differential diagnosis, providing a more accurate understanding of the prognosis, management, and treatment of disorders. It is a nuclear scanning technology based on the tracer principle, by employing small quantities of specific radiopharmaceuticals it measures the emitting annihilation photons of these radioligands.

Specifically, radiotracers used in neurology are often compounds designed to selectively bind to a specific molecular target, a receptor or an enzyme[18]. Radiotracers that target the dopaminergic, serotonergic, and cholinergic receptors are used to study the role of environmental and health factors in mental disorders.

However, pharmacologically active compounds may also be administered with the condition of maintaining the dose below the pharmacologically active one, a practice also known as microdosing [19].

The PET technology is used to analyze changes in blood flow, metabolism, and regional chemical composition. By monitoring the time-dependent distribution of these radiotracers, this technology allows the quantification and visualization of biochemical processes.

Radiotracers that target the CNS must fulfil some requirements to cross the blood-brain barrier (BBB) such as a low molecular weight and a discrete portion of lipid solubility to facilitate this mechanism. However, to exert an effect, the drug shall have an appropriate balance between the lipophilic and hydrophilic properties, as once taken up by the BBB membranes it must partition into the aqueous environment of the brain's interstitial fluid [20]. Moreover, the molecule should bind to the target not only with proper affinity and selectivity but also with physiochemical and pharmacological properties that will ensure safe administration to humans.

Radioligands are made of natural molecules labelled with radioactive isotopes, such as ^{18}F, ^{11}C, ^{15}O, and ^{13}N. The radiotracer's unstable nuclei emit positrons, β^+ particles, which are the antiparticle of the electron. When positron emitters decay a proton turns into a positron, a neutron, and a neutrino. The emitted positron travels a distance before annihilating with an electron from the surrounding area, and the difference between different isotopes is in the energy of emission. When annihilating with a surrounding electron, the positron generates two gamma (γ) rays at 511 keV each with approximately 180° angle.[21] These gamma-emissions are detected by the PET scanner and the data is processed by a computer to create an image of the tracer distribution in the body (Figure 2).

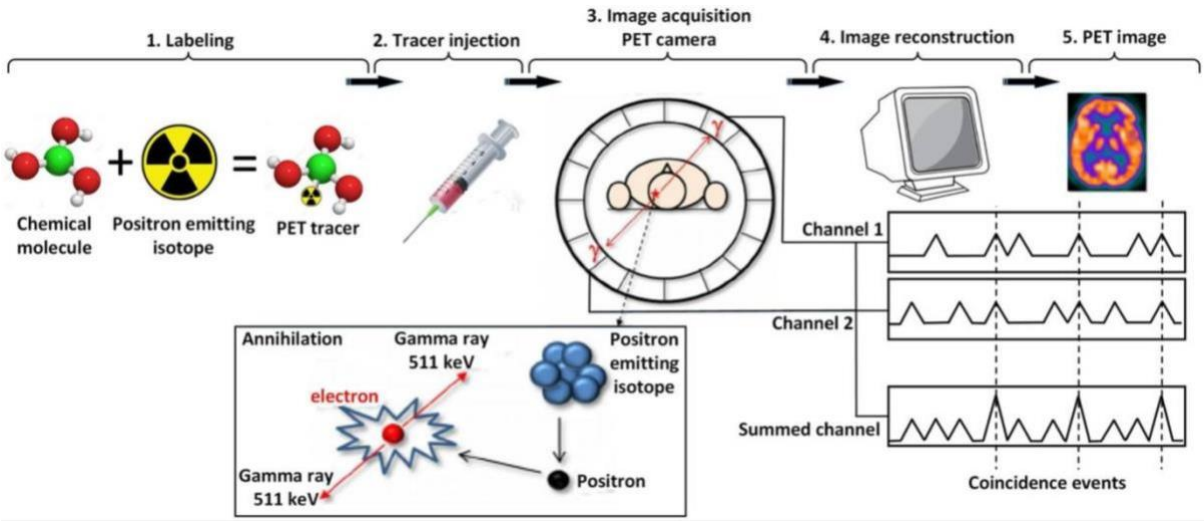

Figure 2. Overview of the labeling of the tracer to the application on humans, data collection, analysis, and development into tomographic images[22]. (Image based on Mohammadi-Nejad, 2018)

Radioactive isotopes are usually generated by a cyclotron (Figure 3) which is a particle accelerator. It works with an electric field that accelerates the ions, usually hydrogen or deuterium (H^- or D^-), and a magnetic field which guides them. To generate the electric field an electric potential difference is applied to the dee and the counter-dee, which are two electrodes connected to the radiofrequency generator. The ion source applied high voltage to H^- or D^- gas, generating negative ions. These ions are extracted from the center of the cyclotron by applying an electrical field. When the electric potential difference is applied, the two electrodes are charged in opposition to one another. The electric field accelerates the ion toward the direction of the dee side as a result. When the ion enters the dee it is affected only by the magnetic field. The ion then leaves the dee and the polarity of the electrodes is reversed, in this situation, the ion is accelerated again towards the counter dee instead. The process is repeated as the orbit radios become higher as well as the speed of the ion. The accelerated particle then spirals towards the border of the magnetic field, reaching a precise value of the radius. When the radius is appropriate, the electrons are removed from the negative ions when they hit a stripping foil. The ion is now positively charged, and it leaves the magnetic field experiencing the same force with the opposite sense. The ion

collides with the target material leading to the final formation of radioactive atoms.[23]

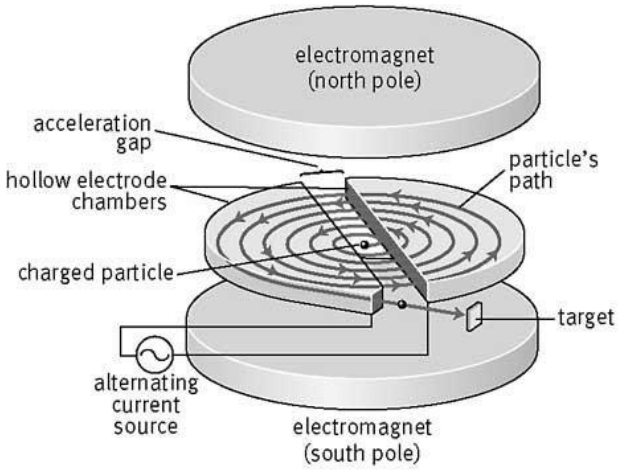

Figure 3[1]**.** Schematic illustration of a cyclotron[2].

PET applied in drug discovery.

It has been estimated by *MEDrays Intell* nuclear medicine world market report 2019, that 39.1% of radiopharmaceuticals and 7% of radiodiagnostics will be used between 2020 and 2025 [24]. This is mainly because PET can be used in precision pharmacology, providing monitoring, and precise information about the development of therapeutic drugs. PET scans can often be used to ensure drug efficacy through biomarkers, or can address the identification of specific/non-specific receptor binding and occupancy, as well as penetration and metabolism in the brain or peripheral metabolism [25]. PET imaging improves the possibility of studying a drug's behaviour by enabling molecular study of a variety of physiological processes.

Moreover, the PET is considered a sensitive and safe imaging method, as it can detect photons from a tracer quantity of radioligand, and it implies a minimum radiation exposure to the patient[26]. Each radioligand, to be eligible as such, should

[1] *I have made every effort to locate all owners of the image rights and have obtained their consent to use the images in this work. Should a copyright infringement nevertheless become known, please notify me.*

meet specific criteria that enable good performances: no active P-glycoprotein mediated efflux pump and receptor density to affinity ratio > 10 are just two examples of these criteria [27].

However, the primary constraint of PET is its limited anatomical information. For this reason, PET is oftentimes coupled with other imaging modalities such as CT or MRI, which on the other hand can provide good anatomical data.

The pathway of a drug

A therapeutic, from its administration, will go through a long pathway until it reaches the target and then it is excreted from the body. The analysis of this process works according to the ADME principle, and it includes the pharmacokinetics of a drug through absorption, distribution, metabolism, and excretion (ADME).

Absorption[28]

The absorption of a chemical is the movement from its site of administration into the bloodstream. There are multiple administration routes available, the main ones are inhalation via the respiratory system, ingestion via the digestive tract, dermal application to the skin or eye, injection through the muscular system or directly into the bloodstream. Several factors influence the rate and the extent of the absorption, the first one being the route of administration, but also the formulation and the chemical properties of the therapeutic.

At the end of the absorption, all compounds must enter the bloodstream therefore intravenously administered drugs are fully bioavailable in the systemic circulation. Other routes of administration may result in incomplete absorption, thus less therapeutic is delivered to the site of action. For example, orally administered drugs will first undergo dissolution in the gastrointestinal tract and then they must cross cell-membranes of the gastrointestinal tract to reach the bloodstream.

Usually, radioligands are directly injected into the bloodstream, ensuring full bioavailability.

Distribution[28]

The distribution refers to the path throughout the body of a drug from the bloodstream to the site of action. The delivery depends on many factors such as blood flow, the degree of binding of the drug to blood and tissue proteins, as well as properties of the molecule (lipid-solubility). Even though vital organs, such as the brain, receive the greatest blood supply, few drugs have a good penetration rate of the CNS. This is because the BBB protects the brain from foreign substances through a complex anatomical structure of the capillary network. Several criteria must be fulfilled to cross the BBB, which be analysed in the next chapter.

Distribution of a therapeutic to its site of action is affected on different levels. It is noteworthy to mention that the blood is composed of red and white blood cells, plasma, and plasma protein, and most drugs bind to plasma protein reversibly. Only unbound drugs can penetrate the tissue membrane therefore the degree to which drugs bind to plasma proteins affects the distribution of the active principle into tissues. Being the process reversible, the affinity of the drug for plasma guides the equilibrium between the amount of drug leaving the bloodstream and the one of drug biding to the plasma proteins.

Metabolism[28]

At this point, drugs can be eliminated either unchanged through the kidneys or, as it happens to most of the drugs, they undergo chemical changes towards more hydrophilic molecules. The liver is the main site of drug metabolism in the human body, and the process toward its metabolites can be generally divided into four phases (0-III).

Phase 0 refers to the cellular uptake of the xenobiotic into hepatocytes. Subsequentially, drugs are modified into more polar compounds by adding oxygen via oxidation, reduction, and hydrolysis reactions (phase I). This step is

mainly catalysed by enzymatic pathways, most often the cytochrome P450 (CYP450) enzyme system is responsible for the process. Phase II describes the conjugation process, which involves the addition of water-soluble molecules to the drug, such as sulfuric acid, acetic acid, amino acid, or glucuronic acid, the most common. In the last phase (phase III) the metabolites are transported out of hepatocytes.

Excretion[28]

The excretion is part of the elimination process together with the metabolism, it aims at the complete removal of the drug from the body through the kidneys. The urine is the main mechanism of drug expulsion. Blood enters the kidneys which act like a strong filter, allowing the passage of only water-soluble compounds dissolved in the urines. If a drug has not been properly converted into a water-soluble compound, it is most likely that it will be reabsorbed into the bloodstream until it is properly modified.

The blood-brain barrier

Tight connections between capillary endothelial cells constitute the highly selective semi-permeable membrane known as the blood-brain barrier (BBB).

The separation between the CNS interstitial fluid from the circulating blood is dynamic; it ensures maintenance of neuronal homeostasis against the everchanging composition and concentration in circulating blood. Its objective, therefore, is to limit the entry of compounds that are essential nutrients or meet the requirements to cross the BBB.

Several cell types collaborate to uphold the integrity and functionality of the BBB, such as the astrocyte, the endothelial cells, pericyte, and the basement membrane, playing a pivotal role in the functioning of the BBB (Figure 4).

The endothelial cells (EC) form a barrier characterized by tight junctions that regulate the passage of molecules.

The pericytes, surrounding the endothelial cells, contribute to regulating the BBB permeability and cerebral blood flow through intricate signalling mechanisms involving astrocytes and neurons.

Astrocytes, multifunctional glial cells, facilitate intercellular communication and provide metabolic support to neurons while influencing the expression of transport protein proteins crucial for BBB function. The basement membrane, situated between pericytes, endothelial cells, and astrocytes, provides both structural support and functional regulation within the perivascular space[29–31].

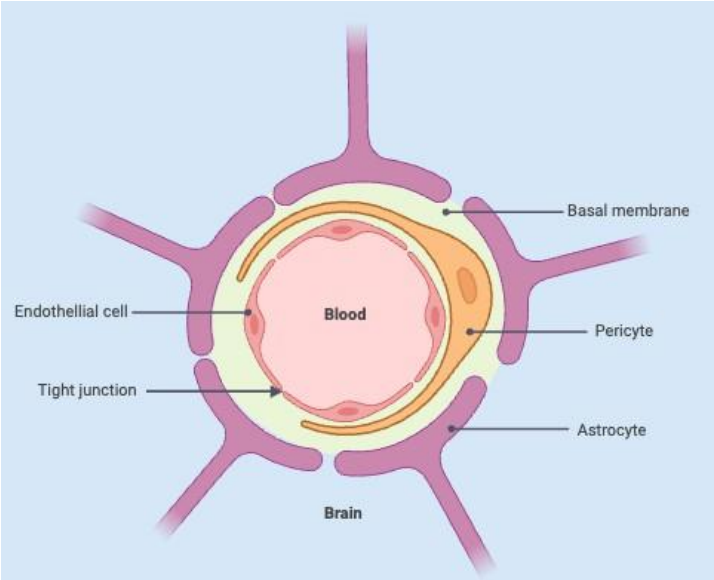

Figure 4. Blood-brain barrier section structure.
(Created with Biorender.com)

The BBB imposes stringent criteria for molecules seeking passage into the brain. Lipid solubility, charge at physiological pH, presence of efflux transporters and protein binding dynamics collectively dictate a molecule's ability to traverse the barrier. Moreover, the balance between total plasma concentration and protein-bound fraction strongly influences the molecule's permeability across the BBB. Various mechanisms facilitate the transport of molecules across the barrier, each tailored to accommodate specific types of substances. Paracellular transport allows water-soluble agents to traverse the intracellular space between endothelial cells, regulated by tight junctions.

More lipophilic compounds exploit the transcellular pathway, diffusing across endothelial cells via passive diffusion. Transport proteins, such as glucose transporters and amino acid carriers, facilitate the passage of essential nutrients via facilitated diffusion. Energy-dependent efflux pumps actively extrude certain substances from the brain, maintaining homeostasis. Receptor-mediated and adsorptive transcytosis mechanisms further enable the selective transport of molecules, often exploited for drug delivery purposes[20,29,31].

Metabolite analysing techniques

PET imaging can reveal details about the target tissue, particularly about its overall radioactivity, however, it cannot reveal its chemical identity.

Radiometabolites detected in the examined tissue might affect the precision of the quantitative analysis of the PET[32].

Considering the multitude of chemical modifications encountered by a radioligand, diverse chemical entities are generated. The concentration of the parental radiotracer drops as the number of products from these biotransformations rises. As previously stated, the PET scanner does not reveal the identity of the pharmacophore; instead, it detects the overall amount of radioactivity in the tissue under examination. Considering these characteristics, radiometabolites can confuse the interpretation of imaging data, therefore, it is fundamental that they are measured and considered in the image quantification.

High-performance liquid chromatography (HPLC) with radioactive detection, radio-HPLC, is the gold standard technique for measuring radioactive metabolites. This technique which is based on the separation of different molecules based on their structure, enables the quantification and identification of various radioactive metabolites with higher resolution. On the other hand, radio-HPLC analysis requires highly trained personnel, high costs due to the expensive equipment and often a large number of solvents used. Besides, the HPLC overall run-time can last up to 10 minutes and longer which leads to

broader and lower peaks due to the dwell time in the column and a poorer determination of compounds with long retention.

The correct method to use a HPLC system, implies a multistep sample preparation ante the injection in the instrument, resulting in time-consuming steps. Considering the short half-life of certain radiotracers, specifically in the final stages of the PET imaging experiments, the combination of these conditions leads to a loss of information.

To overcome these limitations, solid phase extraction (SPE) of the radiometabolites may seem like a reasonable alternative. In this method, the plasma is initially stacked, specifically or after protein precipitation, into the cartridge; the radiotracer and its metabolites are held or extricated from the SPE cartridge based on their chemical behaviour.

Another technique for the determination of radiometabolites is thin-layer chromatography (TLC) in combination with autoradiography. This method is the first chromatographic tool used for the separation of radioactive compounds. It surely is less expensive, easier to apply and faster than the radio-HPLC, but the limitations are in resolution, accuracy, and reproducibility.

Another HPLC technique known as column-switching method [33] works as follows: Plasma is directly loaded onto a capture column and can be separated and removed by retaining the radioactive compounds. By reversing the flow direction and changing the mobile phase, a further separation of the compounds can take place via a downstream separation column. This method reduces time-consuming sample preparation steps, but as a drawback, it suffers from high back pressure to the system due to the large volume of plasma required for radiometabolites analysis, as well as the mandatory cleanliness and frequent cleaning of the entire HPLC system. The positive and negative characteristics of commonly used techniques are shown in Table 1.

Table 1. Advantages and limitations of most used analytical techniques for radiometabolites analysis[34]. (Modified from Ghosh, 2020)

Analytical technique	***Sensitivity***	***Resolution***	***Speed***	***Sample pre-treatment***	***Cost***
Radio-TLC	High	Low	Slow	Yes	Low
Radio-HPLC	High	High	Fast	Yes	High
Column-switching HPLC	High	High	Fast	No	High
SPE	Moderate	Low	Fast	Not always	Low

Principles of radio-HPLC and solid phase extraction

As before mentioned, the HPLC technology is widely used to separate, identify and/or quantify different components of a complex mixture. The separation takes place in a column and it exploits the interactions between a stationary phase and the mobile phase, which is a solvent or a mixture of solvents. The stationary phase is found in the column and is a granular material with small porous particles of different natures. The sample is injected into the mobile phase flow via a valve with a sample loop. The flow then moves from the pump to the analytical column, where the separation takes place. The initial mixture migrates with its different components guided by the interactions with the stationary phase, inducing different retention rates. The components leave the column at different retention times, and the downstream connected radio detector passes the generated signals to a software.

The technology behind the HPLC system is that the solvents are forced through the instrument under high pressures (400-1000 atm).

A modification of the HPLC method is the already mentioned column-switching radio-HPLC, which exploits the technology of a multi-channel switching valve to change the direction of the mobile phase or to change the entire mobile phase. The eluent flows through a primary column (pre-treatment column) and subsequentially through the analysis column at a specific time. The separations

rely on the switching valves that connect the two columns. The pre-purification step aims to enrich the analyte of interest by interfering with impurities. The enriched solution will transfer to the analytical column to complete the specific determination of the compounds.

The solid phase extraction (SPE) method is a combination of liquid chromatography and liquid-solid extraction. It is designed to extract and concentrate target analytes from complex sample matrices, through the selective adsorption and selective elution of the sample components by the solid phase. The concept revolves around the use of a solid sorbent that will interact selectively, retaining specific analytes. Selective retention is achieved through various interactions such as ion exchange or hydrophobic interactions, depending on the nature of the sorbent. After direct loading of the sample on the cartridges, the before-mentioned interactions are used to remove unwanted matrix components through a washing step. Therefore, the solvents used in this step should only interact with interfering compounds without compromising the retained analytes of interest. The target components are eluted from the sorbent in a second step using an appropriate solvent, disrupting the interactions between the sorbent and the analytes. The concentrated and isolated analytes of interest may now undergo other analytical techniques, if necessary, such as chromatography or spectrometry.

Objectives

The primary goal of this project was the optimization and validation of an improved method for metabolite correction out of arterial blood samples.

The published manuscript of Rischka et al. has described a HPLC method for diagnosis of the metabolite analyses to gain metabolite curves out of arterial blood samples to calculate the arterial input function. [35]

Since this described specific HPLC method not only places enormous demands on the device and the personnel, it is also very prone to errors and poor reproducibility is a frequently recurring consequence.

The idea was therefore to achieve simplified chromatographic processing of the blood samples via solid-phase extraction, thereby avoiding the complexity of column chromatography, in particular described "column-switching" method in which plasma is injected directly.

From the available HPLC data, the idea of a work-up via SPE was theoretically feasible, as the retention-time peaks of both radioactive metabolites and the intact tracer *(R)*-[^{11}C]Me-NB1 were very far apart in time. Different analyte conditions must be available for the use of SPE. This is the only way to ensure that this much less precise separation provides reliable results compared to HPLC. In the present case, we were able to observe a temporally good HPLC separation of the peaks from each other of 3-5 minutes, which had been realized on a hydrophilic-lipophilic-balanced (HLB) cartridge and a downstream connected C-18 column.

We started our considerations by using an HLB cartridge with a capacity of 5 mL to obtain as much plasma/radioactivity as possible for the subsequent gamma-counter measurements. The use of different washing solutions or elution solutions was based on the mobile phases from the published HPLC method[35].

To safely elute the two metabolites from the cartridge with two washing steps, but to leave the intact tracer *(R)*-[^{11}C]Me-NB1 on the stationary phase, we used the following solutions:

- Wash solution 1: 1% acetonitrile (ACN) in H_2O

- Wash solution 2: mixture of ACN and 50 mM ammonium acetate (pH 9)

- Elution solution: pure organic solution (ACN or ethyl acetate)

Initially, it was necessary to check whether the unmetabolized radiotracer was not eluted from the cartridge with wash solution 2, but only by the elution solution. For this purpose, we centrifuged fresh whole blood and added a calculated amount of *(R)*-[^{11}C]Me-NB1 to the separated plasma. We eluted into collection tubes which fit to the gamma-counter racks using above mentioned solutions. The tubes were measured for radioactivity and the activity expressed in cpm (counts per minute) was decay corrected (half-life of C-11 is 20.3 min) and plotted.

Building upon the findings, the method was then applied to healthy volunteers to introduce the metabolites to the analysis. At the same time, the effectiveness of the method was counterproofed using the published radio-HPLC method [35].

The secondary objective was to develop a standard operating procedure (SOP) for planned *(R)*-[^{11}C]Me-NB1 studies, that will be available at the General Hospital of the Medical University of Vienna, Department of Biomedical Imaging and Image-guided Therapy, Division of Nuclear Medicine.

EXPERIMENTAL

Materials

- Acetonitrile (99,9%, CAS: 75-05-8, Sigma Aldrich)
- Ammonium acetate (ACS reagent, ≥97%, CAS: 631-61-8, Sigma Aldrich)
- C18 cartridges (reversed-phase Grace® Solid-Phase Extraction, 300 mg, 50 µm, 60 Å)
- Caesium carbonate (Reagent Plus®, CAS: 534-17-8, Sigma Aldrich)
- Dimethyl sulfoxide (ACS reagent, ≥99,9%, CAS: 67-68-5, Sigma Aldrich)
- Dimethylformamide (ACS reagent, ≥99,8%, CAS: 68-12-2 , Sigma Aldrich)
- Distilled water
- Ethanol (EMSURE® ACS,ISO,Reag. Ph Eur)
- Ethyl acetate (ACS reagent, ≥99,5%, CAS: 141-78-6, Sigma Aldrich)
- Gamma counter
- HPLC-column (XBridge Shield RP18; 2.5 µm, 3.0x50 mm)
- [^{11}C]-methyl iodide
- Millex-GV filter (0.22 µm, yellow, Millipore Corporation)
- Oasis HLB Cartridge, 6cc/200mg, 30 µm
- *(R)*-[^{11}C]Me-NB1
- PETtrace cyclotron (GE Healthcare)
- Pyrochrome® chromogenic test kit
- SepPak Plus C18 cartridge
- Tracerlab FX2 C synthesis module (GE Healthcare)
- Vapro Vapor Pressure Osmometer 5600 (Wescor, Sanova Medical Systems)
- Veenstra VDC404 Radioisotope Dose Calibrator

- Methrom 913 pH meter
- XSelectTM column (HSST3, 3.5 µm, 100x 4.6 mm)

Synthesis of *(R)*[^{11}C]Me-NB1

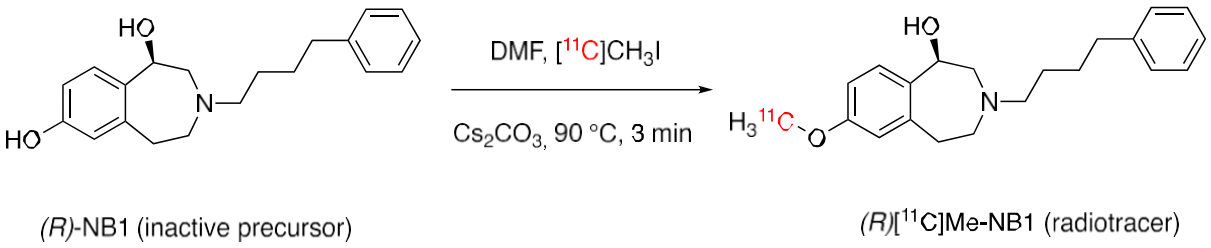

(R)-NB1 (inactive precursor)

(R)[^{11}C]Me-NB1 (radiotracer)

The synthesis of *(R)*-[^{11}C]Me-NB1 is fully automated and performed using Tracerlab FX2 C synthesis module (GE Healthcare), a commercially available, fully automated synthetic unit to produce ^{11}C- methylated PET tracers (Figure 5). The synthesis has been well established, and it consists of several steps, beginning with the production of [^{11}C]carbon dioxide in the PETtrace cyclotron. [^{11}C]CO_2 is converted into [^{11}C]methyl iodide through a gas phase reaction, inside the Tracerlab FX2 C synthesizer module. The reaction of the 3-((1R,2S)-2-amino-1-hydroxypropyl)phenol (1.0 mg) and Cs_2CO_3 (2.0 mg) dissolved in 500 µL DMF with [^{11}C]methyl iodide (3 min, 90°C) to give *(R)*-[^{11}C]Me-NB1. The crude mixture is purified in the cell with a semi-preparative HPLC. The solvents are then removed using a solid phase extraction technique with a SepPak Plus C18. The cartridge is washed with 10 mL of water and eluted with 1.5 mL of ethanol and sodium chloride solution (0.9%, 5 mL). The final purified product is then filtrated under aseptic conditions on a sterile filter (Millex-GV filter (0.22 µm, yellow, Millipore Corporation).

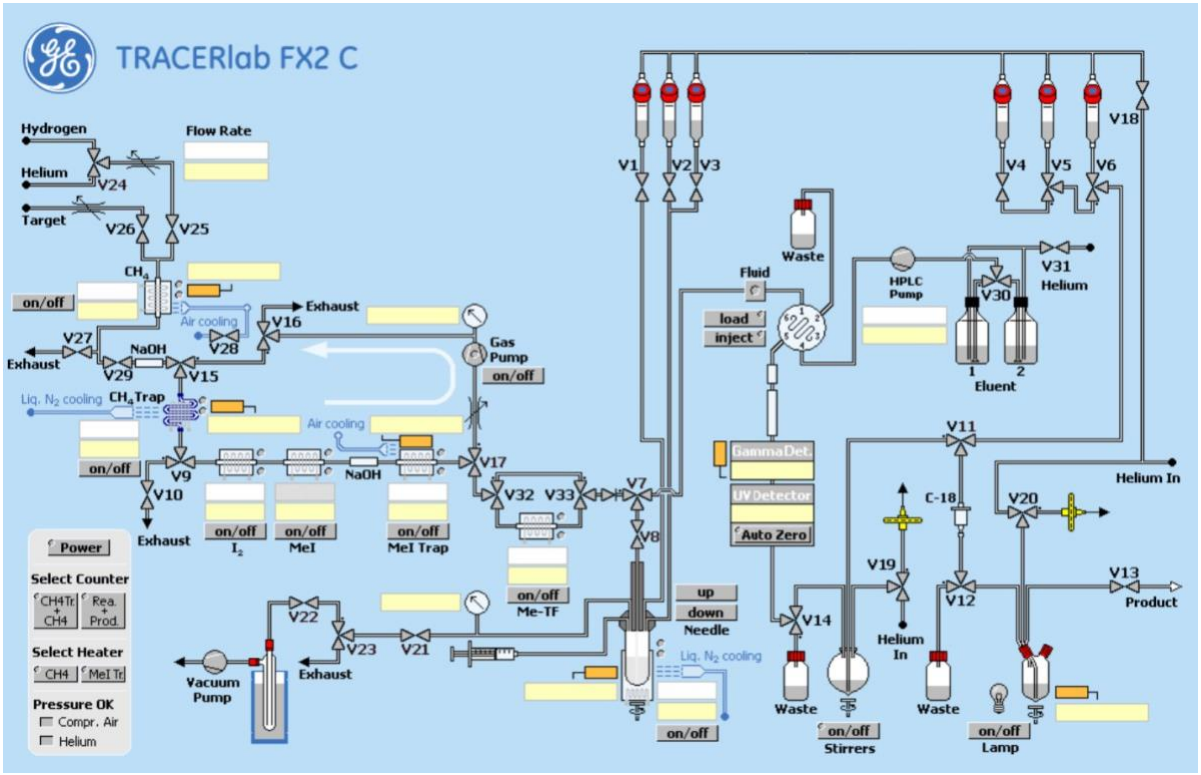

Figure 5. TRACERlab FX2 C synthesizer module.

Quality Control (QC)

Each batch of *(R)*-[^{11}C]Me-NB1 undergoes quality control before release to the patients, only the bacterial endotoxins and sterility test are performed after each production due to a parametric release of short-lived radiotracer according to the cGRPP guidelines[36]. All QC tests have been performed according to the SOPs available at the Medical University of Vienna.

- Radionuclidic purity is determined by (1) the Gamma-spectrum which shows a sole peak at 430-520 keV and (2) by calculating the physical half-life which is 20.3 ±2 min. The half-life is measured at different time points using a Veenstra VDC404 Radioisotope Dose Calibrator and calculation is made through the following equation:

$$T_{1/2} = -\ln 2 \cdot (t_2 - t_1) / \ln \frac{A_2}{A_1}$$

Where A_1 is the starting activity at t_1 and A_2 is the end activity at t_2.

- Radiochemical purity and chemical purity are measured with radio-HPLC. A chromatogram of *(R)*-[^{11}C]Me-NB1 and desmethyl-NB1 (precursor) as reference is recorded before analysis of the radioactive product. A 5 µL aliquot is manually injected into the HPLC. The retention time of the radioactivity peak must correspond to the retention time of the reference (radiochemical identity).

  The retention time for *(R)*-[^{11}C]Me-NB1 is 1.95 min and for desmethyl-NB1 1.15 min. The UV signals are used for the determination of the chemical purity. The percentage of *(R)*-Me-NB1 peak (RI channel) corresponds to the radiochemical purity and should be ≥95%. The calibration curve covers the concentration range of 1-10 µg/mL. the HPLC has a limit of detection (LOD) of 1.9 µg/mL. In the case of not-detectable amounts of product within the UV channel, the molar activity is calculated with the LOD.

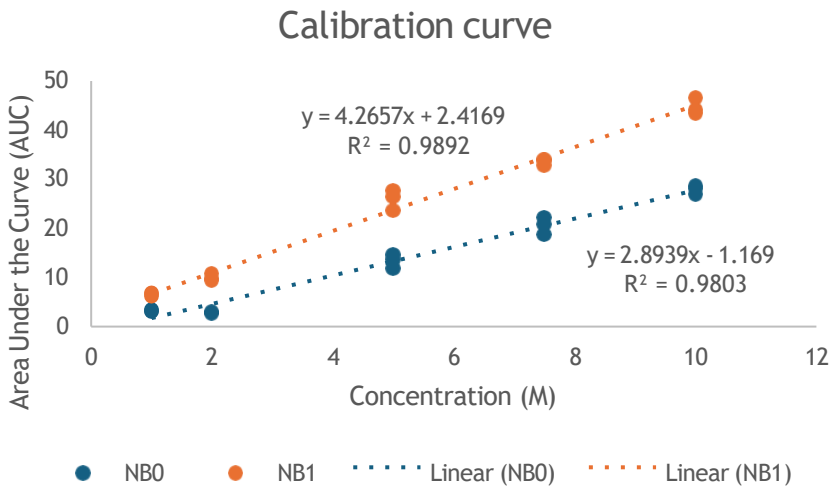

The set-up used for the HPLC includes a column XBridge Shield RP-18; 3.0 x 50 mm; 2,5 µm particle size column. The mobile phase consists of:

A: 100 mM ammonium phosphate + 5 mM sodium-1-octansulfonat, B:

acetonitrile/water (90/10 v/v), C: Aqua bidest. And D: 50 mM ammonium phosphate (pH 9.3). Flow rate: 1 mL/min; UV wavelenght: 230 nm.

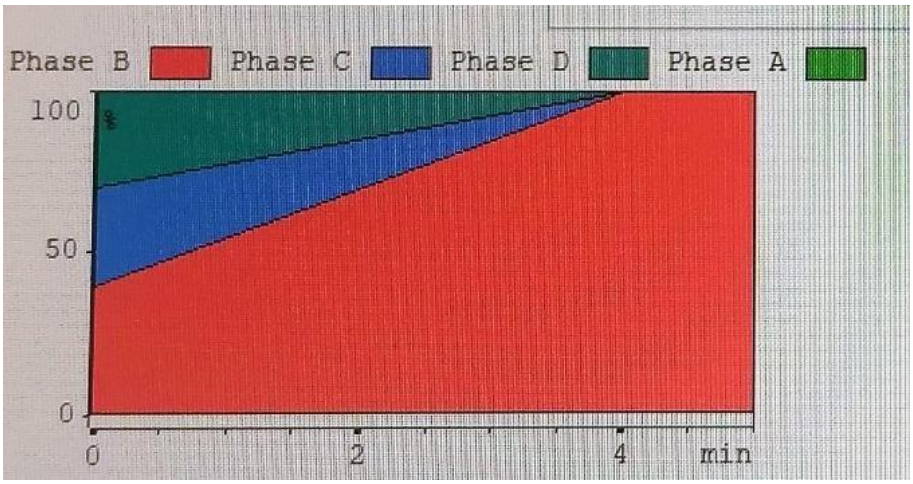

Figure 6. HPLC gradient program

- Residual solvent analysis is performed by gas chromatography (GC) with flame ionisation detector (FID) (carrier gas: He, flow 2.7 mL/min, 45 °C (2.5 min); 20 °C/min to 110 °C; 30°C/min to 200 °C; 200 °C 10 min); FID: 270 °C). A 30 µl aliquot is drawn from the Eppendorf® vial containing *(R)*-[^{11}C]Me-NB1 injection aliquot and added to an autoinjector vial. The limit is 5000 ppm for DMSO and 400 ppm for ACN[37].
- The pH of *(R)*-[^{11}C]Me-NB1 is determined with a Metrohm 913 (Metrohm Inula GmbH, Vienna, Austria).
- The osmolality of an aliquot of the PET tracer is measured in a Vapro Vapor Pressure Osmometer 5600 (Wescor, Sanova Medical Systems, Vienna, Austria).
- Bacterial endotoxin tests are conducted at a GMP-certified laboratory according to European Pharmacopoeia (MPL–Mikrobiologisches Prüflabor GmbH, Innsbruck, Austria). A kinetic assay using a Pyrochrome® chromogenic test kit is used (Method D Ph. Eur.). The detection limit of this method is 0.05 E.U./mL. According to the Ph. Eur. 1999, 1325

monograph and according to Ph. Eur. 2000, 125 “Radioaktive Arzneimittel” the endotoxin test may be performed after the release of the PET drug.

- Sterility testing as well as the bacterial endotoxins test can be performed after the PET release. The sterility is performed on a 1 mL aliquot of each produced batch of *(R)*-[^{11}C]Me-NB1 after radioactive decay. Until the test is performed the solution is stored at 4 °C. and these are conducted at MPL, accordingly.

Administration to the patient and blood collection

This pilot study involving healthy subjects aims to optimize the analysis method of metabolites by using SPE instead of published HPLC method [27] and, therefore, does not encompass any imaging procedures. Six healthy volunteers were recruited for this study. During a single visit, a target dose of 6 MBq/kg body weight of *(R)*-[^{11}C]Me-NB1 was administered intravenously by a qualified physician. Recognizing the concerns associated with radiomedicine, medical experts were readily available throughout the entire study to address any queries or concerns from the participants. Participants retained the right to withdraw from the pilot study without any consequences on their medical care. For reasons of patient comfort and simplification of the process, venous blood was chosen for sampling instead of arterial blood, as arterial blood was not required for the establishment of the SPE method. Furthermore, a PET scan was not part of the analysis method and was therefore not performed. The blood samples, totalling 9 mL, were collected by the physician at defined time intervals: 5 min, 10 min, 20 min, 40 min, 60 min, and 80 min post-administration. These samples were immediately brought to the metabolite laboratory for further analysis.

Sample analysis

Cartridges and preconditioning

The chosen cartridges to conduct the set-up of the analytical analysis are Oasis HLB Cartridges, 6cc/200 mg, 30 µm (Waters, Austria), as well as Grace® C18 cartridges, 300 mg, 50 µm, 60 Å (Fisher Scientific, Schwerte, Germany). HLB cartridges are made from the hydrophilic N-vinylpyrrolidone and the lipophilic divinylbenzene, in a specific ratio of the monomers. The C-18 cartridge is based on the principle of the reversed-phase SPE cartridge. It uses a non-polar adsorbent (carbohydrate or polymer) on the stationary phase to separate the organic solute from the polar phase. Van der Waals interactions between non-polar substances are the driving force of this technique, and the affinity of the adsorbent to the solute mainly depends on its hydrophobicity. The stationary phase of the SPE cartridge consists of hydrophobic C18 (Octadecyl) functional groups chemically bonded to the silica backbone.

Each cartridge used in the experiments has been pre-conditioned with 5 mL of EtOAc, 5 mL EtOH and 5 mL of distilled water.

Sample pre-treatment

An aqueous solution of 8 % phosphoric acid has been prepared in advance and it has been used to acidify plasma before loading to the HLB cartridge. The ratio of plasma/ phosphoric acid was set to 4:1.

0.2 mL of whole blood (WB) were pipetted into pre-weighed polypropylene (PP) vials, which were measured for radioactivity on the Gamma counter. Simultaneously, the collection vial underwent centrifugation (4°C, RFC 3504, 4 min), resulting in the separation of approximately 5 mL of plasma. After centrifugation, 0.2 mL of plasma was withdrawn, pipetted in PP vials and counted accordingly.

Loading of the samples

Pre-conditioned cartridges were then loaded with 5 mL of plasma/ 8% phosphoric acid mixture, connected to a needle (0.4 mm ID) and eluted in vacuum collecting tubes by piercing through their septa.

Elution and collection

Following cartridge loading and eluting to the first collection tube, 5 mL of a prepared solution containing 1% ACN in H_2O was loaded to the empty cartridge and eluted to the second collection vial.

The subsequent step which was the loading of an ACN/ AmAc (pH 9) ratio was the main investigation and focused on determining the optimal ratio between ACN and AmAc (pH 9) to prevent the elution of *(R)*-[^{11}C]Me-NB1 into the tube 3 while permitting the sole elution of metabolites. Initially, a broad range of ACN/AmAc (pH 9) ratios were explored, as mentioned in the table (Table 2). Finally, 100% ACN was used to elute the parental compound collected in tube 4 (see Figure 6).

Table 2. Schematic description of loading, washing and elution steps

	Loading	**Liquid composition**	**Eluted compound**
Tube 1	5 mL of sample	Plasma/ 8% phosphoric acid (4:1)	Hydrophilic metabolite
Tube 2	5 mL wash solution 1	1% ACN in H_2O	
Tube 3	5 mL wash solution 2	ACN/ AmAc (pH 9)[a]	Less hydrophilic metabolite
Tube 4	5 mL eluent	100% ACN or EtOAc	Parent compound *(R)*-[^{11}C]Me-NB1

[a]*In tube 3, different ratios of ACN/ AmAc (pH 9) were used: 10/90, 20/80, 30/70, 40/60,50/50, 60/40*

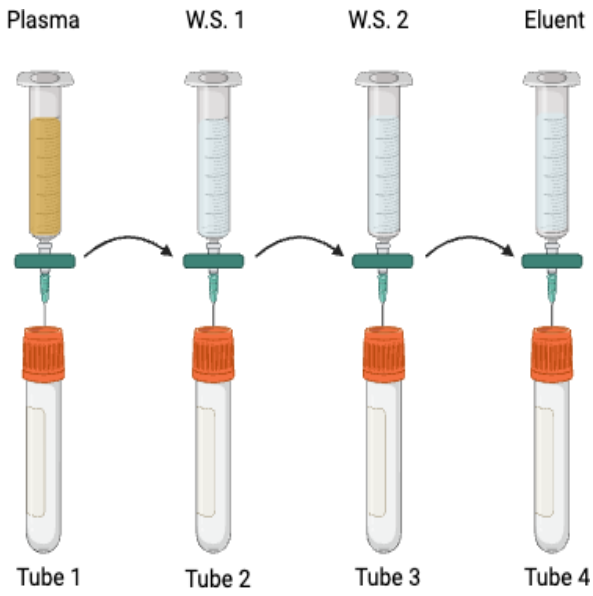

Figure 6. Visual description of the set-up. The syringe is initially loaded with plasma, and collected in tube 1. Hydrophilic radioactive metabolites pass through, while less hydrophilic or more lipophilic metabolites, as well as the tracer (R)-[^{11}C]Me-NB1 retain in the cartridge. For subsequential loading as well as elution steps the same syringe and needle is used for elution on all continuing tubes. (Created with Biorender.com)

Gamma counter

Initially, gamma radiation measurements of both whole blood (WB) and plasma were conducted at each designated time point. Subsequently, tubes 1-4 underwent gamma radiation measurement using the Gamma counter. The resulting data were then decay corrected and graphically plotted to facilitate the informed selection of the optimal solution for tube 3.

The decay correction has been calculated using the following formula:

$$A_t = A_0 \cdot e^{-\lambda \Delta t}$$

A_t = activity at time *t*

A_0 = initial activity

$\lambda = \frac{\ln 2}{T^{1}/_{2}}$

Δt = time elapsed

Radio-HPLC

To ensure the robustness of the newly developed cartridge method, it was subjected to a comparison to the radio-HPLC method published by Rischka et al. (2022). Specifically, the content of tubes 3 and 4 were scrutinized by spiking the injection solution with *(R)*-Me-NB1 reference standard. The conditions of the radio-HPLC method were described elsewhere [35].

RESULT AND DISCUSSION

The project's outset concentrated on refining and validating an improved SPE method for quantitatively separating *(R)*-[^{11}C]Me-NB1 and produced metabolites. The principal knowledge of enzymatically formed metabolites and remaining radiotracer in the region of interest is of utmost importance for the subsequent calculated metabolite correction to determine the occupancy of radiotracer in the investigated region. The objective was to streamline chromatographic processing through solid-phase extraction, eliminating the intricacies associated with column chromatography, specifically the complex radio-HPLC method [22], in which a "column-switching" step is included as well as the involving direct plasma injection.

The first question to be answered was whether the radiotracer can be reliably and quantitatively recovered exclusively in the last elution step (tube 4) from a blood sample spiked with *(R)*-[^{11}C]Me-NB1 using the cartridge separation method. For this purpose, the radiotracer *(R)*-[^{11}C]Me-NB1 was introduced into ex-vivo blood samples.

The blood sample was centrifuged (described above) and the separated plasma spiked with *(R)*-[^{11}C]Me-NB1. Additionally, the plasma was then acidified with 8% phosphoric acid (4:1 plasma/phosphoric acid) according to the manufacturer's instructions, which should improve the separation performance of the HLB cartridge. The elution steps were then carried out according to the set-up. As the

plasma has no hydrophilic metabolising enzymes for *(R)*-[^{11}C]Me-NB1 which is based on the publication of Rischka et al. (2020), it was assumed according to the elution protocol, that the activity would be quantitatively found in the last tube.

In view of the fact that the focus is on metabolite analysis and not on determining the whole blood/plasma ratio, the measurement of these aliquots, which was additionally carried out, was not continued in order to focus on the experimental setup for cartridge separation.

In detail, it was that the plasma was loaded on six HLB cartridges (5 mL of acidified plasma per cartridge), and each was eluted in tube 1. When the cartridges were empty, they were moved to tube 2, where 5 mL of 1% ACN in H_2O washed out hydrophilic metabolites as well as other impurities of the HLB cartridges. Solutions with a range from 10/90 up to 60/40 of ACN/ AmAc (pH 9) were previously prepared and added to the cartridges for collection to tube 3. For the final step, 5 mL pure ACN was added to the cartridges to elute in tube 4.

It was expected that with increasing lipophilicity of the wash solution 2, *(R)*-[^{11}C]Me-NB1 would start to elute into tube 3. For this purpose, we approached the point of increasing ACN content in the elution solution.

Through this preliminary analysis, it was observed that using up to 20% ACN for washing solution 2, less than 1.2% of *(R)*-[^{11}C]Me-NB1 was observed in tube 3. The elution of *(R)*-[^{11}C]Me-NB1 into tube 3 starts significantly raising when the ACN percentage reaches 30% (Figure 7). This finding guided the subsequent experiments limiting the threshold of ACN to 20%.

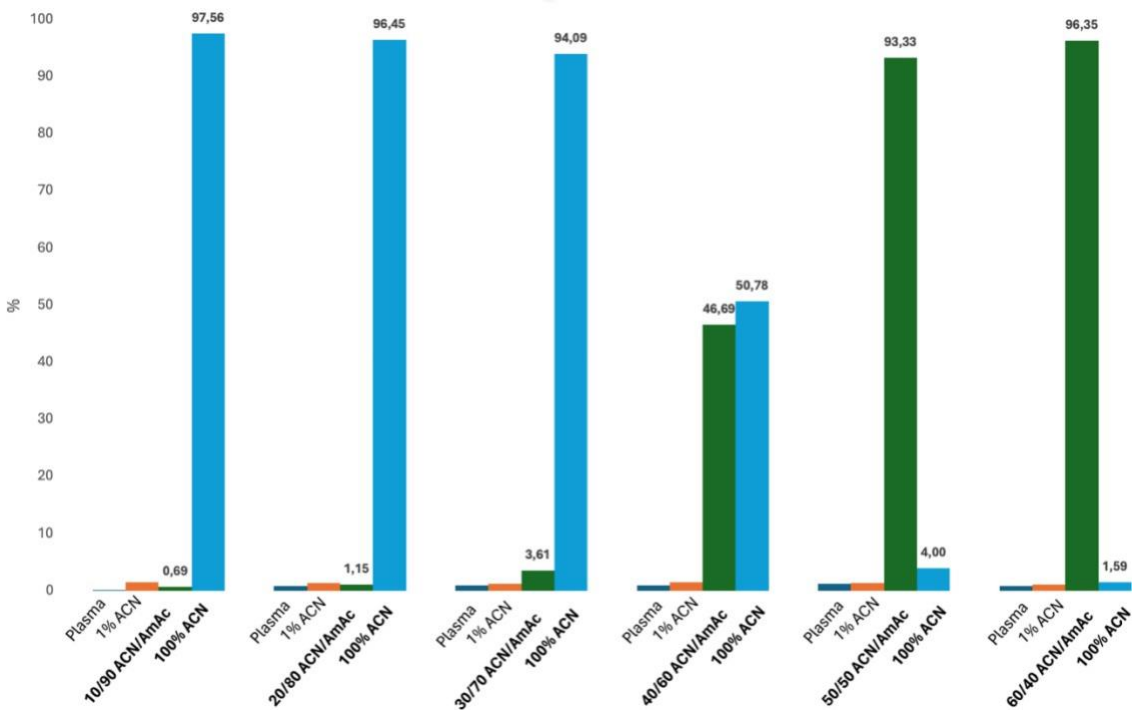

Figure 7. With the increase in lipophilicity, the trend reverses as expected. Until 20% of ACN is used as wash solution 2 (WS2), *(R)*-[^{11}C]Me-NB1 is less than 1.2% eluted. An increase of 10% of ACN, starts the elution-boost of the parent compound in tube 3.

For a more accurate approximation, we have decided to change the proportion of ACN in 2% steps from 12/88 ACN/ AmAc (pH 9) to the mentioned maximum of ratio 20/80 ACN/ AmAc (pH 9) in each batch (Figure 8).

It should not go unmentioned, that we also tried to improve the elution strength of ACN in this step. For this purpose, we tried to use EtOAc instead of ACN in the last step, which was observed in the improved recovery in step 4.

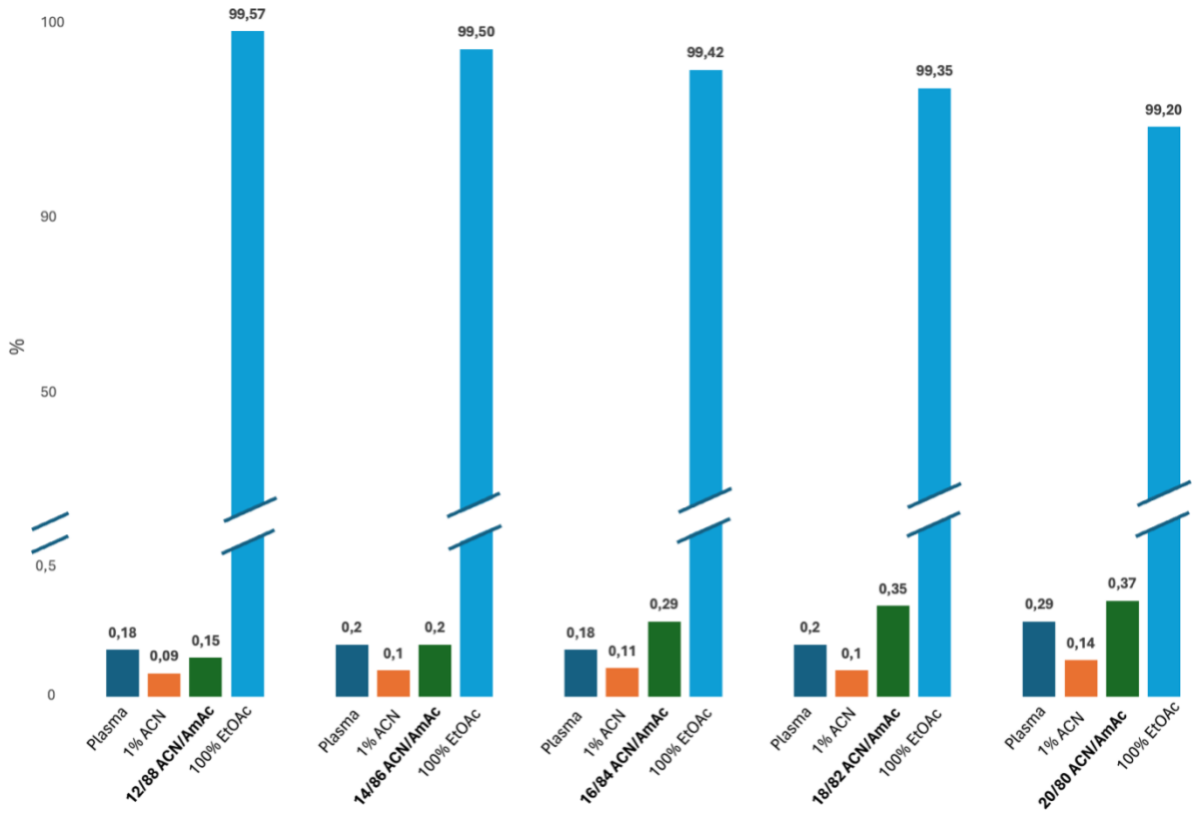

Figure 8. The set of ratios of ACN/AmAc (pH 9) used in this experiment shows that until 20% of ACN is used as WS2, there is the correct environment to avoid the elution of the parent compound in tube 3.

In the following experiments, however, we went back to ACN and refrained from using EtOAc, as its immiscibility with aqueous solutions can lead to 2-phase solutions, which can also influence its use in the HPLC used later for comparison.

Considering the positive results obtained in this experiment, we decided to begin the second step of the project and include the administration of *(R)*-[^{11}C]Me-NB1 to healthy volunteers. In this part, the volunteers were administered with the PET tracer *(R)*-[^{11}C]Me-NB1 by a physician and blood was sampled at fixed time points. Initially, we were interested in investigating blood samples at minutes: 5', 10', 20', 40', 60', 80' as it was evaluated by Rischka et al. (2022). It was decided to focus on the set-up, thus no HPLC comparing method has been used during this first experiment. Considering the previously positive results with a low percentage

of ACN, in this case, a ratio of 10/90 was initially used. Due to the known metabolic profile[35] which shows a significant decrease and inversely increase of *(R)*-[^{11}C]Me-NB1 and radioactive metabolites over time, we would ideally expect such progress using our method.

Once the separation cartridge is in an aqueous environment after preconditioning, the hydrophilic metabolite is eluted both for the first elution step (acidified plasma) in tube 1 and 1% ACN in water for tube 2. As a result, it is found in both tubes and is subsequently summarised as Plasma+WS1 as shown in Table 2. The primary focus in this evaluation step is to focus on the correct separation of the parent compound *(R)*-[^{11}C]Me-NB1 from the second metabolite. Experiments performed with 10% ACN as wash solution 2, showed less than 1.2% of activity detected in collection tube 3 (Table 3), whereas both the plasma and WS1 (more hydrophilic) as well as the eluent (more lipophilic) solutions showed higher activity. This may suggest that the metabolite formation of the less hydrophilic metabolite is more slowly in comparison to the more hydrophilic one.

Table 3. Results using 10/90 ACN/ AmAc (pH 9) as wash solution 2.

HLB-cartridge	***Solution***	***mL***	***5 min***	***10 min***	***20 min***	***40 min***	***60 min***	***80 min***
			%					
1	**Plasma+WS1**	5.0	13.27	31.66	52.78	71.07	79.65	55.63
	WS2	5.0	0.92	1.16	1.14	1.17	1.17	1.66
	Eluent	5.0	85.81	67.18	46.08	27.76	19.18	39.06
2	**Plasma+WS1**	5.0	7.42	14.15	44.43	39.87	56.08	47.40
	WS2	5.0	0.78	0.43	0.80	1.50	0.95	1.66
	Eluent	5.0	91.81	85.42	54.77	58.62	42.98	50.93
3	**Plasma+WS1**	5.0	1.53	2.78	9.20	14.69	20.90	23.48
	WS2	5.0	0.43	0.66	0.84	0.94	1.26	1.41
	Eluent	5.0	98.04	96.56	89.96	84.37	77.84	75.11

All three experiments showed the expected trend for plasma and WS1 as well as the eluent. The hydrophilic metabolites increased with time (depending on their grade of lipophilicity), whereas the parent compound decreased as it is metabolized. Nevertheless, the most lipophilic metabolite did not elute solely with the wash solution 2 but with the eluent which showed us to further modify WS2.

In contrast with our hypothesis, this assumption does not go along with the radio-HPLC data from the HPLC setup experiments of 2020, which took place for the publication of Rischka et al., where the less hydrophilic metabolite was significantly higher than we observed throughout our experiments.

To qualitatively test the power of the described SPE method as well as to figure out the reason for above mentioned inconsistencies, the published HPLC method of Rischka et al. [35] was simultaneously used to give us information on the separation of metabolite(s) and *(R)*-[^{11}C]Me-NB1. A reference standard (10-50 µg/mL) was used throughout the experiments as a proof of concept and to show the corresponding UV-peak to the radiotracer *(R)*-[^{11}C]Me-NB1. The sample was initially prepared with 3 mL of ACN (eluent for tube 4) and mixed with 2 mL of HPLC mobile phase (60:40 ACN:AmAc (pH 9)), for a total amount of 5 mL to be injected in the HPLC. The chromatograms obtained from the analysis of tube 4, showed that the current set-up was not retaining the compounds with the desired strength. In fact, from the beginning of the experiment, at minute 5, the chromatogram of the 4th tube showed a very wide peak (RT=01'17) which remained present also in the chromatograms of minutes 10 and 20 (Figure 9).
This result clearly showed us that the retention of the metabolites as well as (R)-[^{11}C]Me-NB1 cannot be massively influenced by increasing the organic content in solution 2. The ability of an HLB phase is that it retains lipophilic and hydrophilic components well in both aqueous and organic solvents.

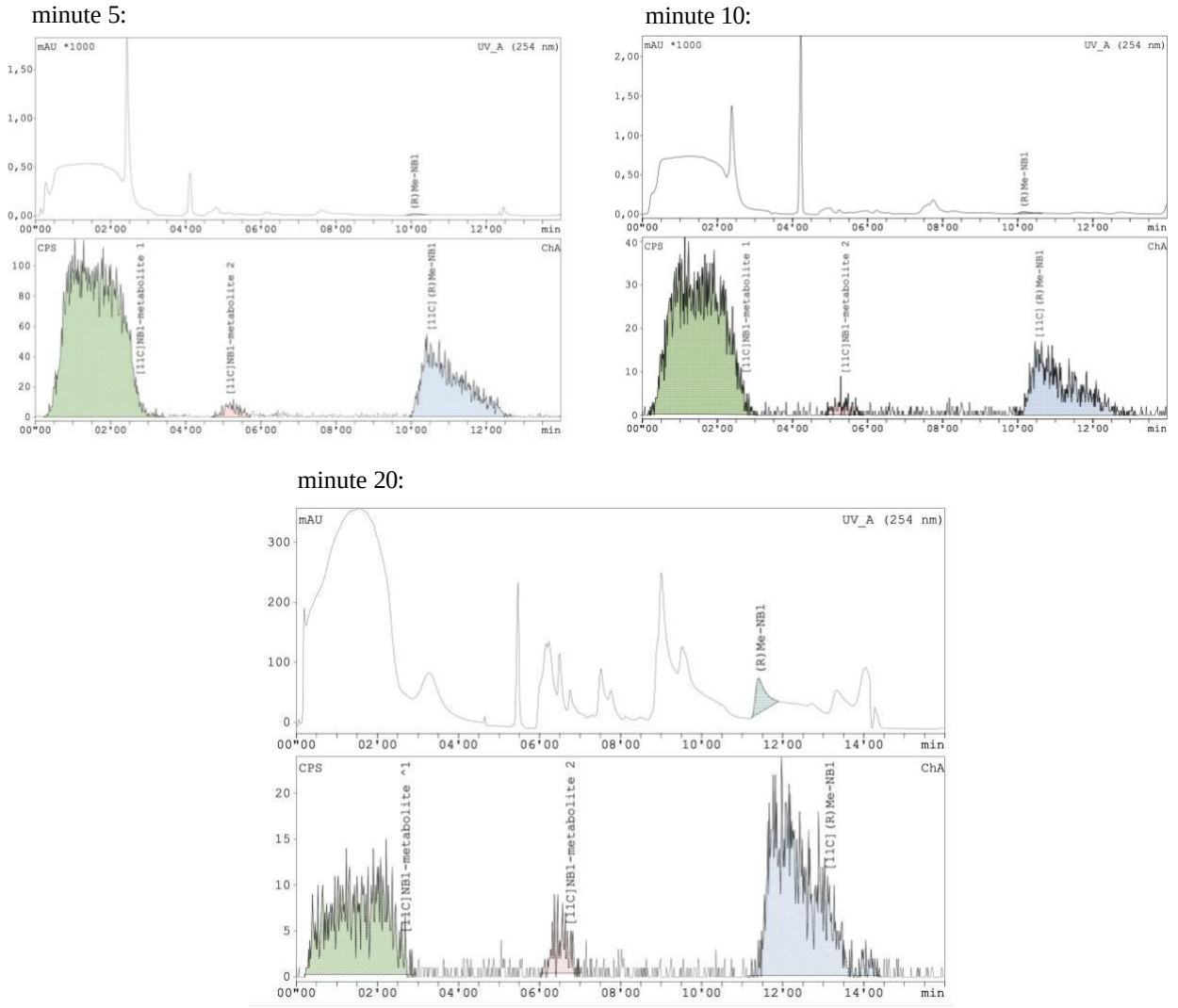

Figure 9. Chromatograms of the HPLC analysis of tube 4 at minutes 5, 10, and 20. Even if there is an increment of the parent compound (RT = 10’33), the modification of the set-up used for the SPE cartridges does not separate properly the compounds as assumed.

This information suggested that we had to change the stationary phase for better results. A C-18 phase instead of the HLB phase came into play. We decided on C-18, since the second HPLC-column of the column-switching-based method of Rischka et al. (2022), which separates the second metabolite and (R)-[^{11}C]Me-NB1 is using this kind of stationary phase.

Besides, the injected solution was too lipophilic and most of the compounds of interest were running with the front of the solvent, which was shown in not

reproducible results and chromatograms with very broad and not separated peaks eluting with the dead time of the HPLC. The reason for this phenomenon was, that the total ACN amount in the 5 mL injection volume which was calculated to be 84%, justifying the unretained elution and the lack of separation. Therefore, during the following experiments we tried to limit ACN as a part of the injection solution to a small amount, resulting in an improvement of the separation. The best and most comprehensible results were finally given by reducing the ACN content to nearly or even zero, which goes along with the published method and purely injected plasma, which is pure aqueous.

To preserve the injection samples as pure aqueous, it was needed to remove the organic portion of the eluted tubes 3 and 4 as much as possible and subsequently resuspend it with an aqueous phase. The samples underwent a heating/drying process processed with an aluminium heating block at 100°C under a nitrogen stream.

By applying this step, separation improvements as well as better-shaped peaks were observed in the chromatograms (Figure 10). These findings go along with the retention times of the HPLC method evaluation for the publication of Rischka et al. [35]

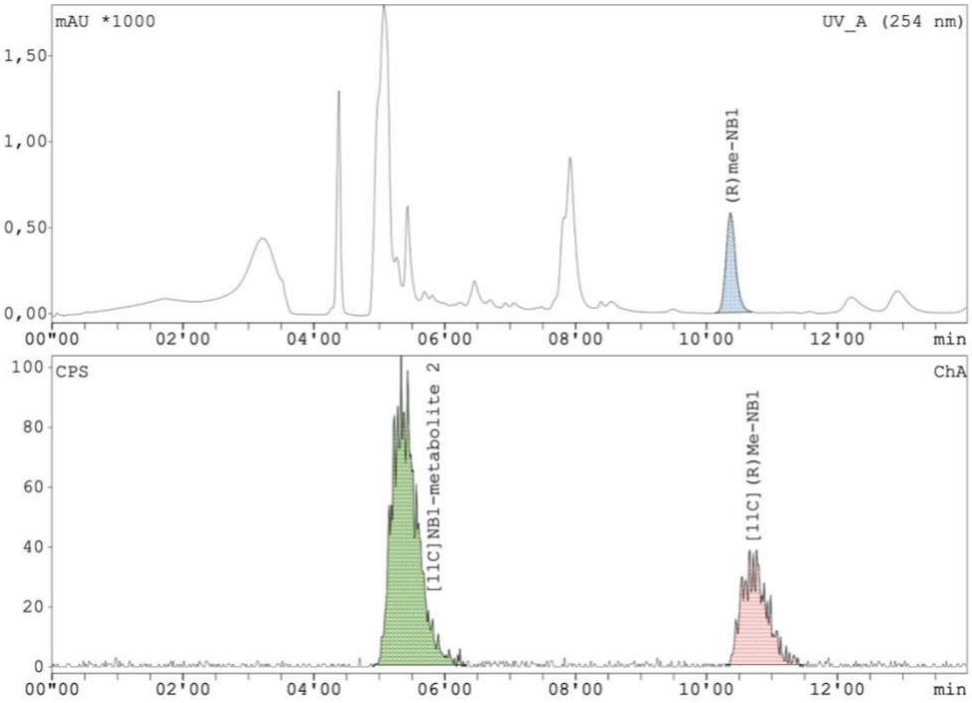

Figure 10. The ACN content was significantly reduced with a heating/drying process, leading to an improvement in the HPLC results.

The set-up of the HPLC method of Rischka et al [35], starts with an HLB cartridge, flushed with an almost pure aqueous mobile phase. The injected less hydrophilic metabolites as well as the radiotracer *(R)*-[^{11}C]Me-NB1 are trapped but not the more hydrophilic compound, which is immediately shown as a radioactive peak on the chromatograms. The column is then back-flushed by reversing the flow direction using a different, more organic solvent composition to release the trapped compounds from the SPE-column and separate the less hydrophilic metabolite from *(R)*-[^{11}C]Me-NB1 on a downstream connected C18 column.

Based on this setup we reconsidered our plan. This was based on the contradictory findings of the nearly quantitative recovery of *(R)*-[^{11}C]Me-NB1 in tube 4 when

having an ACN/ AmAc (pH 9) ratio of 10/90 (ex-vivo test with no metabolization) but not with metabolized blood from volunteers using the same ratio for tube 3.
Since HLB, stands for hydrophilic-lipophilic-balanced, we initially hypothesized that both metabolites as well as *(R)*-[^{11}C]Me-NB1 are leaving the column differently by changing the mobile phase composition which is obviously predetermined by the column characteristics. However, the restraining or elution of the components in this type of stationary phase is different to the known characteristics of a C18 phase, for example.

Due to time constraints, we decided to simultaneously run and compare the separation quality of HLB cartridge directly to a C18 cartridge. The dried and pure AmAc (pH 9) buffer resuspended eluates from both tube 3 and tube 4 were analysed using the HPLC method of Rischka et al. to check the content of metabolites and *(R)*-[^{11}C]Me-NB1 in these fractions.
Since the C-18 column does not need to acidify the plasma before adding, the overall radioactivity in the sample was higher. Consequently, we could reduce the cartridge volume to 3 mL compared to 5 mL of the HLB cartridge by having a comparable activity in the solution.
This direct comparison of the two cartridge types showed us that we could establish the method more quickly because, as mentioned above, the behaviour of the cartridge in relation to different ratios of organic solution and buffer was more predictable for us. We therefore decided to switch after a further changing of the solution ratio, followed by a repeated no-satisfying outcome from the HLB-cartridge completely to the C18 cartridge and to continue our further evaluation with this type only.

We had to adapt the ratio of the washing solution 2, to obtain a better separation of the metabolites to *(R)*-[^{11}C]Me-NB1 because we did not observe a strict separation using the HPLC method. By using the ratio 10/90 ACN:AmAc (pH 9)

for tube 3, too much metabolite was visible in tube 4, therefore we raised the organic content to 20/80. Moreover, considering that our interest was solely on the metabolite separation, we reduced the time points of blood sampling and chose those when metabolite growth was already significant. We decided to collect at time points 10', 20', and 40'.

With these conditions, a separation improvement was registered on the HPLC method. which was addressed to the C18 cartridge. For the HLB cartridge no improvement was seen, which goes along with the discussed different behaviour of this type of stationary phase (Table 4). Therefore, we continued focusing on optimizing the WS2 ratio using solely the C18 cartridge.

Table 4. Comparison between HLB and C18 cartridges

Minute	**Solution**	**HLB (%)**	**C18 (%)**
10'	Plasma+WS1	35.31	59.62
	WS2[a]	3.04	6.84
	Eluent	61.66	33.54
20'	Plasma+WS1	54.67	71.99
	WS2	6.29	8.29
	Eluent	39.04	19.71
40'	Plasma+WS1	-	77.00
	WS2	-	5.00
	Eluent	-	18.00

[a]WS2 has a ratio of 20/80 ACN:AmAc (pH 9) buffer.

After the solvent ratio of 20/80 ACN/AmAc (pH 9) was still not sufficient for the C18 cartridge, we changed it to 30/70 and higher. In the subsequent analysis, we increased the ratio up to 35/65 ACN/AmAc (pH 9). At this ratio, there was already too much ACN in the mixture, which led to a slight elution of *(R)*-[^{11}C]Me-NB1 to tube 3.

Finally, the solvent ratio of 30/70 was satisfactory and showed a 1.5% carryover of metabolites to tube 4. The 98.5% recovery of *(R)*-[^{11}C]Me-NB1 in tube 4 was therefore sufficient for further analyses and we finalised the evaluation phase using this setup (Figure 11).

Tube 3 minute 30:

Tube 4 minute 30:

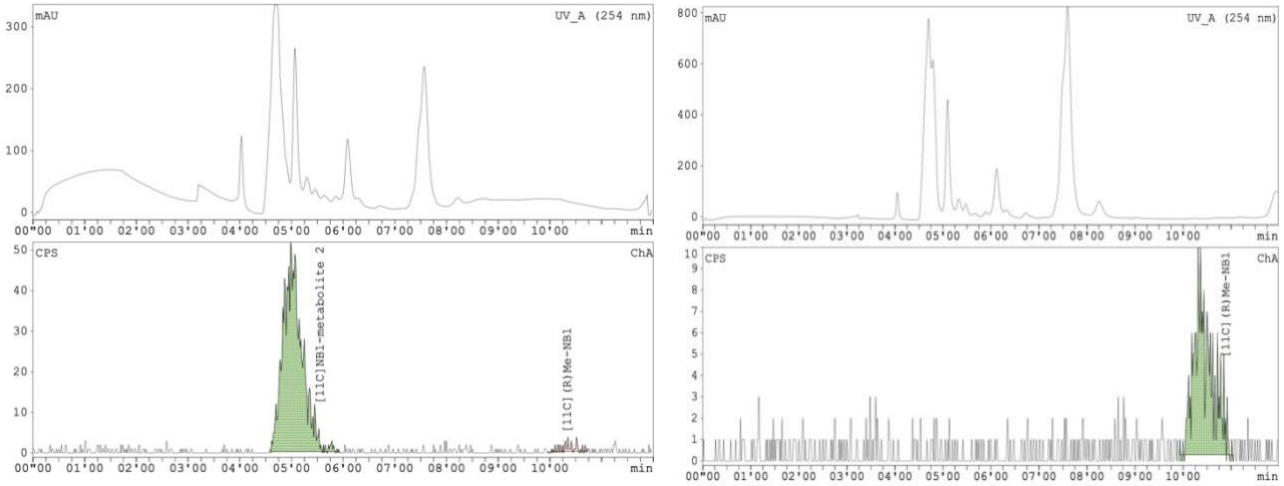

Figure 11. The last set-up used (30/70 ACN/AmAc (pH 9)), shows on the chromatogram a satisfactory starting point for the study of the separation between *(R)*-[^{11}C]Me-NB1 and its metabolites.

CONCLUSION

During this master's thesis project, we wanted to address the complexity, error-proneness, and poor reproducibility associated with the existing HPLC method for metabolite correction from arterial blood samples[35] generated from the metabolism of the radioligand, *(R)*-[^{11}C]Me-NB1. The solution presented in this project prompts the optimization and validation of a simplified chromatographic processing method via solid-phase extraction to improve both the accuracy and reliability of the method. The solid-phase extraction is a commonly used method in the analysis of plasma, because of its low costs and the simplicity of it.

The set-up of this project was initially based on the data available from the previous HPLC data. The method was based on the column-switching method, which was realized on a hydrophilic-lipophilic-balanced (HLB) cartridge and a downstream connected C-18 column. Therefore, we decided to begin with the HLB cartridges loaded with plasma and washed with two different solutions to collect the metabolites, and finally, the elution of the cartridge would collect the unmetabolized parent compound.

The different washing solutions or elution solutions were initially based on the mobile phases from the HPLC method. During the first part of the project, the radioligand *(R)*-[^{11}C]Me-NB1 was added to collected blood samples, thus there wasn't metabolite production. Here, we have identified the ideal percentage range of lipophilicity to collect the unmetabolized *(R)*-[^{11}C]Me-NB1 in one batch. In the second part of the thesis, we introduced the administration of the radioligand to the volunteers and a comparison with the C-18 cartridges to overcome the lack of precision found with the HLB cartridges.

From this comparison, we decided to continue with the C-18 cartridges as the process was significantly simpler compared to HLB cartridges, as well as we obtained higher precision. Therefore, the C-18 cartridges were chosen to continue with the study, and we identified an ideal percentage needed between the

hydrophilicity and lipophilicity of the solutions to have an optimal separation between the metabolites and *(R)*-[^{11}C]Me-NB1.

The results obtained during the development of a simpler and more precise method for metabolite correction of the radioligand *(R)*-[^{11}C]Me-NB, were promising. Certainly, the work done during this master project has laid the groundwork for a substantial optimization effort of the method. In the future, a broader study should be carried on for both refining and validating the method using the solid-phase extraction with C-18 cartridges.

References

1. Gallo, S., Vitacolonna, A. & Crepaldi, T. NMDA Receptor and Its Emerging Role in Cancer. *Int. J. Mol. Sci.* **24**, 2540 (2023).
2. El-Saftawy, A. A. M. REGULATING THE PERFORMANCE PARAMETERS OF ACCELERATED PARTICLES.
3. Traynelis, S. F. *et al.* Glutamate Receptor Ion Channels: Structure, Regulation, and Function. *Pharmacol. Rev.* **62**, 405–496 (2010).
4. Hadzic, M., Jack, A. & Wahle, P. Ionotropic glutamate receptors: Which ones, when, and where in the mammalian neocortex. *J. Comp. Neurol.* **525**, 976–1033 (2017).
5. Cull-Candy, S. G. & Leszkiewicz, D. N. Role of Distinct NMDA Receptor Subtypes at Central Synapses. *Sci. STKE* **2004**, (2004).
6. Nowak, L., Bregestovski, P., Ascher, P., Herbet, A. & Prochiantz, A. Magnesium gates glutamate-activated channels in mouse central neurones. *Nature* **307**, 462–465 (1984).
7. Paoletti, P. & Neyton, J. NMDA receptor subunits: function and pharmacology. *Curr. Opin. Pharmacol.* **7**, 39–47 (2007).
8. Karakas, E. & Furukawa, H. Crystal structure of a heterotetrameric NMDA receptor ion channel. *Science* **344**, 992–997 (2014).
9. Vicini, S. *et al.* Functional and Pharmacological Differences Between Recombinant *N* -Methyl- D -Aspartate Receptors. *J. Neurophysiol.* **79**, 555–566 (1998).

10. Cull-Candy, S., Brickley, S. & Farrant, M. NMDA receptor subunits: diversity, development and disease. *Curr. Opin. Neurobiol.* **11**, 327–335 (2001).

11. Furukawa, H. Mechanisms of activation, inhibition and specificity: crystal structures of the NMDA receptor NR1 ligand-binding core. *EMBO J.* **22**, 2873–2885 (2003).

12. Rischka, L. *et al.* Biodistribution and dosimetry of the GluN2B-specific NMDA receptor PET radioligand (R)-[11C]Me-NB1. *EJNMMI Res.* **12**, 53 (2022).

13. Wyllie, D. J. A., Livesey, M. R. & Hardingham, G. E. Influence of GluN2 subunit identity on NMDA receptor function. *Neuropharmacology* **74**, 4–17 (2013).

14. Sun, Y. *et al.* The Functional and Molecular Properties, Physiological Functions, and Pathophysiological Roles of GluN2A in the Central Nervous System. *Mol. Neurobiol.* **54**, 1008–1021 (2017).

15. Vieira, M., Yong, X. L. H., Roche, K. W. & Anggono, V. Regulation of NMDA glutamate receptor functions by the GluN2 subunits. *J. Neurochem.* **154**, 121–143 (2020).

16. Franchini, L., Carrano, N., Di Luca, M. & Gardoni, F. Synaptic GluN2A-Containing NMDA Receptors: From Physiology to Pathological Synaptic Plasticity. *Int. J. Mol. Sci.* **21**, 1538 (2020).

17. Berti, V., Pupi, A. & Mosconi, L. PET/CT in diagnosis of dementia. *Ann. N. Y. Acad. Sci.* **1228**, 81–92 (2011).

18. Suridjan, I., Comley, R. A. & Rabiner, E. A. The application of positron emission tomography (PET) imaging in CNS drug development. *Brain Imaging Behav.* **13**, 354–365 (2019).

19. Ozenil, M. *et al.* Update on PET Tracer Development for Muscarinic Acetylcholine Receptors. *Pharmaceuticals* **14**, 530 (2021).

20. Pardridge, W. M. Drug Transport across the Blood–Brain Barrier. *J. Cereb. Blood Flow Metab.* **32**, 1959–1972 (2012).

21. Turkheimer, F., Veronese, M., Dunn, J. *Experimental Design and Practical Data Analysis in Positron Emission Tomography*. (CreateSpace Independent Publishing Platform, 2014).

22. Mohammadi-Nejad, A.-R. *et al.* Neonatal brain resting-state functional connectivity imaging modalities. *Photoacoustics* **10**, 1–19 (2018).

23. Strijckmans, K. The isochronous cyclotron: principles and recent developmentsq. *Comput. Med. Imaging Graph.* (2001).

24. Nerella, S. G., Singh, P., Sanam, T. & Digwal, C. S. PET Molecular Imaging in Drug Development: The Imaging and Chemistry Perspective. *Front. Med.* **9**, 812270 (2022).

25. Rudin, M. & Weissleder, R. Molecular imaging in drug discovery and development. *Nat. Rev. Drug Discov.* **2**, 123–131 (2003).

26. James, M. L. *et al.* New Positron Emission Tomography (PET) Radioligand for Imaging σ-1 Receptors in Living Subjects. *J. Med. Chem.* **55**, 8272–8282 (2012).

27. Honer, M., Gobbi, L., Martarello, L. & Comley, R. A. Radioligand development for molecular imaging of the central nervous system with positron emission tomography. *Drug Discov. Today* **19**, 1936–1944 (2014).

28. Vrbanac, J. & Slauter, R. ADME in Drug Discovery. in *A Comprehensive Guide to Toxicology in Nonclinical Drug Development* 39–67 (Elsevier, 2017). doi:10.1016/B978-0-12-803620-4.00003-7.

29. Abbott, N. J. Blood–brain barrier structure and function and the challenges for CNS drug delivery. *J. Inherit. Metab. Dis.* **36**, 437–449 (2013).

30. Abbott, N. J., Patabendige, A. A. K., Dolman, D. E. M., Yusof, S. R. & Begley, D. J. Structure and function of the blood–brain barrier. *Neurobiol. Dis.* **37**, 13–25 (2010).

31. Wu, D. *et al.* The blood–brain barrier: structure, regulation, and drug delivery. *Signal Transduct. Target. Ther.* **8**, 217 (2023).

32. Price, J. C. *et al.* Analyses of [^{18} F]altanserin bolus injection PET data. II: Consideration of radiolabeled metabolites in humans. *Synapse* **41**, 11–21 (2001).

33. Hilton, J. *et al.* Column-switching HPLC for the analysis of plasma in PET imaging studies. *Nucl. Med. Biol.* **27**, 627–630 (2000).

34. Ghosh, K. K. *et al*. Dealing with PET radiometabolites. *EJNMMI Res.* **10**, 109 (2020).

35. Rischka, L. *et al.* First-in-Humans Brain PET Imaging of the GluN2B-Containing *N* -methyl-d-aspartate Receptor with (*R*)- ^{11} C-Me-NB1. *J. Nucl. Med.* **63**, 936–941 (2022).

36. Gillings, N. *et al.* Guideline on current good radiopharmacy practice (cGRPP) for the small-scale preparation of radiopharmaceuticals. *EJNMMI Radiopharm. Chem.* **6**, 8 (2021).

37. Guide for the elaboration of monographs on radio-pharmaceutical preparations.

Appendix

SOP

Metabolite analysis for *(R)*-[^{11}C]Me-NB1 using solid phase extraction (SPE)

1. **APPLICATION AREA**

   This SOP is valid at the General Hospital of the Medical University of Vienna, Department of Biomedical Imaging and Image-guided Therapy, Division of Nuclear Medicine. The SOP describes the method to perform metabolite correction out of arterial blood samples, using SPE.

2. **RELATED DOCUMENTS**

   N.D.

3. **RESPONIBILITIES**

   N.D.

4. **ABBREVIATIONS**

   Acetonitrile (ACN)
   Ammonium acetate (AmAc) pH 9
   Polypropylene (PP)
   Washing solution (WS)
   Whole blood (WB)

5. **REQUIRED MATERIAL**

   ACN
   AmAc
   C18 cartridges (reversed-phase Grace® Solid-Phase Extraction, 300 mg, 50 µm, 60 Å)
   Distilled water
   Ethanol
   Methanol
   Gamma counter

(R)-[^{11}C]Me-NB1

Polypropylene vials (5 mL, 75x12 mm)

VACUETTE® TUBE (6 mL, Z 13x100 mm)

XSelectTM column (HSST3, 3.5 µm, 100x 4.6 mm)

6. PROCEDURE

Preparation of the solutions and cartridge conditioning Prepare in advance all the needed solutions in a 50 mL Greiner tube: 50 mM of ammonium acetate buffer (pH 9); washing solution 1 with 1% ACN in distilled H_2O; washing solution 2 with 30/70 ACN and ammonium acetate buffer; and the eluent (100% ACN).

For each timepoint, prepare on a rack four vacuum-sealed collecting tubes and one cartridge each equipped with its own needle. One cartridge/needle is needed for each timepoint (6 cartridges). Label all the tubes and cartridges with the relative timepoints and separation step (for the tubes: Plasma, WS1, WS2, Eluent)

Blood is sampled at minutes: 5', 10', 20', 40', 60', 80'.

Precondition the cartridges using 5 mL of ACN, 5 mL of EtOH and 5 mL of distilled water.

When the blood arrives, pipette 0.2 mL of WB into pre-weighed polypropylene (PP) vial and measure it on the Gamma counter for radioactivity. Simultaneously, put the collection-vial under centrifugation (4°C; RFC 3504, 4 min), resulting in the separation of approximately 5 mL of plasma. After centrifugation, withdraw 0.2 mL of plasma in a pre-weighed PP vial, proceed for counting on the Gamma counter and weight the vials again (WB and plasma).

For each timepoint proceed as described:

Load the cartridge with 3 mL of plasma, connect the needle to the cartridge and penetrate it to the first vacuum-sealed collecting tube. When no more fluid flushed through the needle, withdraw the cartridge/needle from the septum of tube 1, load the cartridges with 3 mL of WS 1 and place the cartridge/needle to the second collecting tube. Subsequently, proceed with 3 mL of WS 2 and connect the needle to the third tube; finally elute tube 4 with 3 mL of ACN. When the first collecting vials are filled, remove the caps, and place them on a gamma-counter rack for measurement.

Label the print-out papers after counting with the corresponding positions of every single tube in the rack.

To graphically plot data obtained with the Gamma counter, apply the decay correction on the CPM values using the following formula:

$$A_t = A_0 \cdot e^{-\lambda \Delta t}$$

A_t = activity at time *t*

A_0 = initial activity

$\lambda = \frac{\ln 2}{T^1/_2}$

Δt = time elapsed

7. REVISION

Date	Version	Description of revision
30.04.2024	01	Creation and release